Norepinephrine-induced small GTPase RHOB mediates nocturnal intraocular pressure rise in mice

Authors

Keisuke Ikegami[1,2*], Takumi Takahashi[1], Yuto Katamoto[1], Atsuro Oishi[3], Akihide Yoshimi[4], Miki Nagase[3], Atsuya Miki[5], Shinobu Yasuo[1], Satoru Masubuchi[2]

Author affiliations

[1] Laboratory of Regulation in Metabolism and Behavior, Faculty of Agriculture, Kyushu University, 744 Motooka, Nishi-ku, Fukuoka, 819-0395, Japan

[2] Department of Physiology, School of Medicine, Aichi Medical University, 1-1 Yazako-karimata, Nagakute, Aichi, 480-1195, Japan

[3] Department of Anatomy, Kyorin University Faculty of Medicine, Tokyo, Japan

[4] Division of Cancer RNA Research, National Cancer Center Research Institute, Tokyo, Japan

[5] Department of Myopia Control Research, Aichi Medical University, 1-1 Yazako-karimata, Nagakute, Aichi, 480-1195, Japan

*Correspondence: Keisuke Ikegami, Ph.D.

Laboratory of Regulation in Metabolism and Behavior, Faculty of Agriculture, Kyushu University, 744 Motooka, Nishi-ku, Fukuoka, 819-0395, Japan

Phone: +81 92 802 4598

Email: ikegami.keisuke.271@m.kyushu-u.ac.jp

Supplementary information

Table of Contents

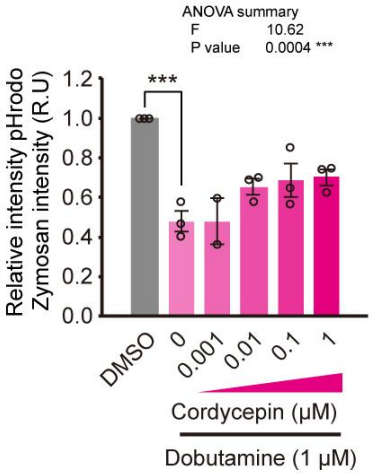

Supplementary Figure 1: Involvement of transcription in norepinephrine (NE)-suppressed TM phagocytosis.

Transcription inhibitor cordycepin partially rescued dobutamine-induced TM phagocytosis suppression (***$p < 0.001$, Dunnett's multiple comparison, one-way ANOVA [$p = 0.0004$]). Data are normalized by signals of DMSO-treated cells and presented as bar graphs (mean ± SEM) with scatter plot of independent experiments (n = 3).

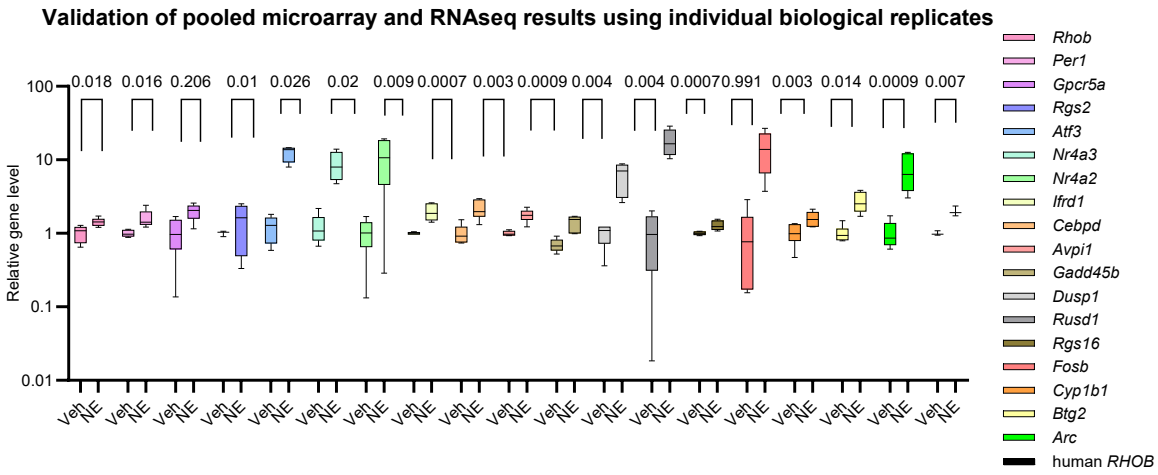

Supplementary Figure 2: qRT-PCR validation of NE-induced RHOB-related transcriptomic changes in mouse eyes and human TM cells.

Eighteen genes identified as overlapping candidates between the pooled mouse eye microarray dataset and the human trabecular meshwork RNA-seq dataset were examined by qRT-PCR using RNA isolated from individual mouse eyes following NE treatment (n = 5 [Veh], n = 6 [NE]). RHOB and most candidate genes were significantly upregulated by NE stimulation, confirming the reproducibility of the pooled mouse eye microarray findings in independent biological samples. In addition, qRT-PCR analysis using RNA from NE-treated iHTMCs confirmed NE-induced upregulation of *RHOB* under the same 6-h treatment condition used for RNA-seq analysis (n = 3 per group). Gene expression levels were normalized to *Hprt* for mouse eye samples and to *HPRT1* for iHTMC samples, and expressed relative to the vehicle-treated group. Box plots show the median and interquartile range, with whiskers indicating the minimum and maximum values. Statistical significance was determined using Welch's t-test.

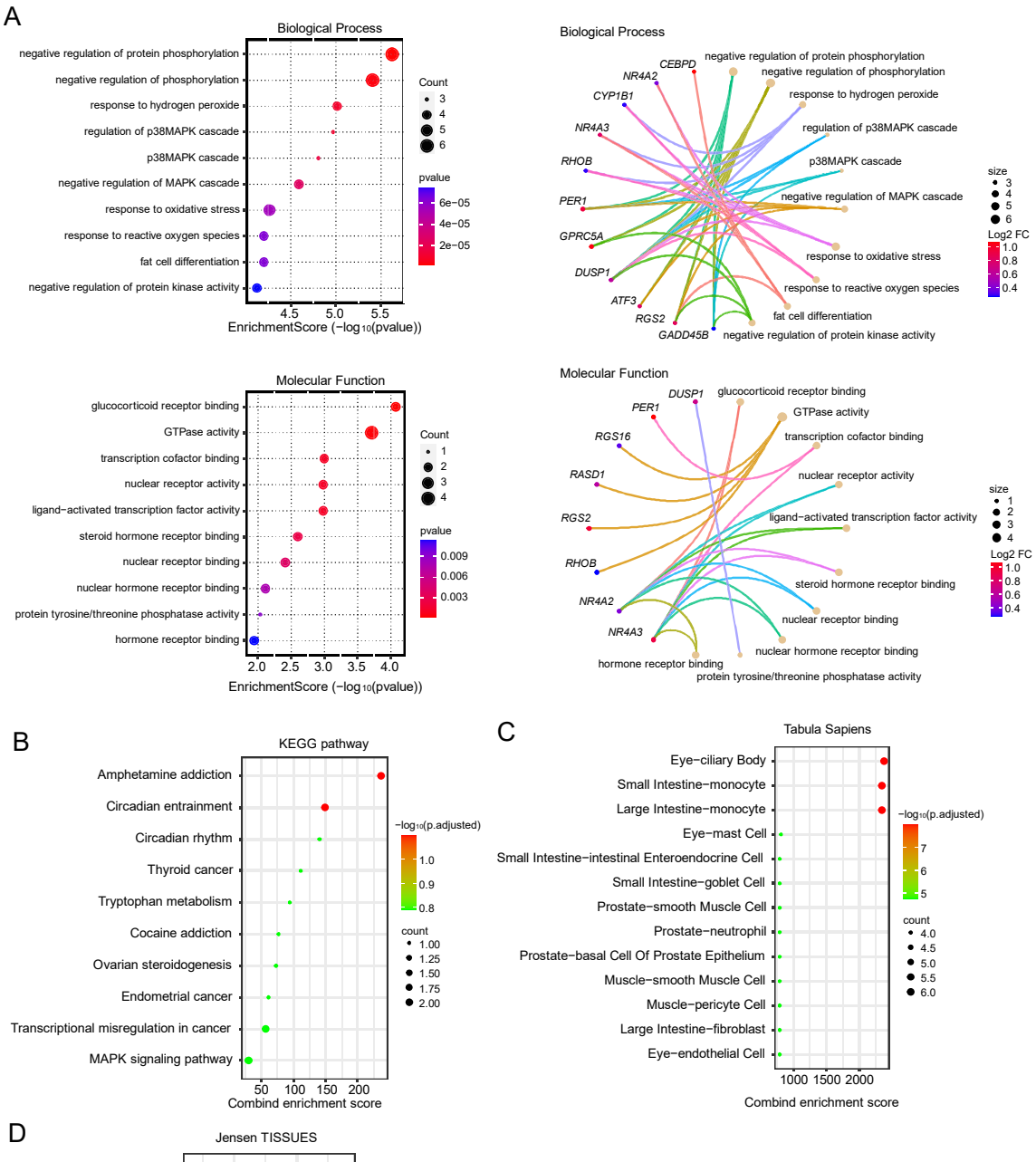
A
Biological Process
negative regulation of protein phosphorylation
negative regulation of phosphorylation
response to hydrogen peroxide
regulation of p38MAPK cascade
p38MAPK cascade
negative regulation of MAPK cascade
response to oxidative stress
response to reactive oxygen species
fat cell differentiation
negative regulation of protein kinase activity
Count
pvalue
EnrichmentScore (−log10(pvalue))
Molecular Function
glucocorticoid receptor binding
GTPase activity
transcription cofactor binding
nuclear receptor activity
ligand−activated transcription factor activity
steroid hormone receptor binding
nuclear receptor binding
nuclear hormone receptor binding
protein tyrosine/threonine phosphatase activity
hormone receptor binding
CEBPD
NR4A2
CYP1B1
NR4A3
RHOB
PER1
GPRC5A
DUSP1
ATF3
RGS2
GADD45B
size
Log2 FC
RASD1
B
KEGG pathway
Amphetamine addiction
Circadian entrainment
Circadian rhythm
Thyroid cancer
Tryptophan metabolism
Cocaine addiction
Ovarian steroidogenesis
Endometrial cancer
Transcriptional misregulation in cancer
MAPK signaling pathway
−log10(p.adjusted)
count
Combind enrichment score
C
Tabula Sapiens
Eye−ciliary Body
Small Intestine−monocyte
Large Intestine−monocyte
Eye−mast Cell
Small Intestine−intestinal Enteroendocrine Cell
Small Intestine−goblet Cell
Prostate−smooth Muscle Cell
Prostate−neutrophil
Prostate−basal Cell Of Prostate Epithelium
Muscle−smooth Muscle Cell
Muscle−pericyte Cell
Large Intestine−fibroblast
Eye−endothelial Cell
D
Jensen TISSUES
Ganglion
Adrenal cortex
Spinal cord
Ophthalmic nerve
Olfactory bulb
Pineal gland
Corpus callosum
Eye
Superior cervical ganglion
Pancreatic islet

Supplementary Figure 3: Enrichment analysis of upregulated 18 genes.

(**A**) Gene ontology (GO) enrichment analysis of the 18 DEGs. The top ten (ranked by p-value) significantly enriched GO terms in the biological process and molecular function groups for each gene are shown. Pearson's correlation matrix of GO enrichment analysis of DEGs. GTPase activity is associated with multiple genes. Larger symbols indicate a greater number of genes correlated with the GO term. (**B**) KEGG pathway analysis revealed that the amphetamine addiction and the circadian entrainment were likely induced by NE in iHTMC. (**C**) Tabula Sapiens analysis revealed that upregulated 18 genes were likely expressed in eye-ciliary body. (**D**) Jensen TISSUES analysis revealed that upregulated 18 genes were likely expressed in the ganglion and the adrenal cortex, related to NE.

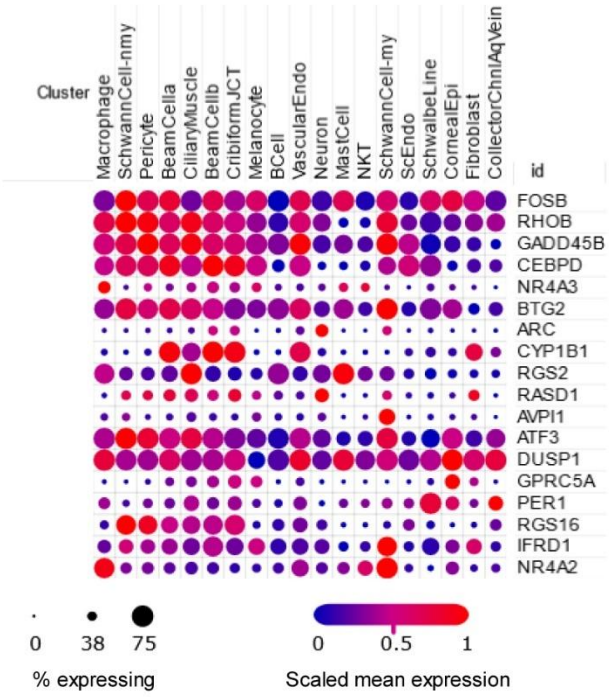

Supplementary Figure 4: Gene expressions of upregulated 18 genes in human AH outflow-related cells

FOSB, *RHOB*, *GADD45B*, *CEBPD*, *BTG2*, *RGS2*, *ATF3*, *DUSP1*, and *NR4A2* were expressed in TM macrophages. In particular, *RHOB* levels were higher than those of circadian related *PER1* and *RGS16*. TM cell types: BeamCella, BeamCellb, and CribiformJCT; macrophages: TM macrophages; corneal epithelium: CornealEpi; myelinating Schwann cell: SchwannCell-my; nonmyelinating Schwann cell: SchwannCell-nmy; vascular endothelium: VascularEndo; Schlemm canal endothelium: ScEndo.

Fig. 2E Western blots full membranes

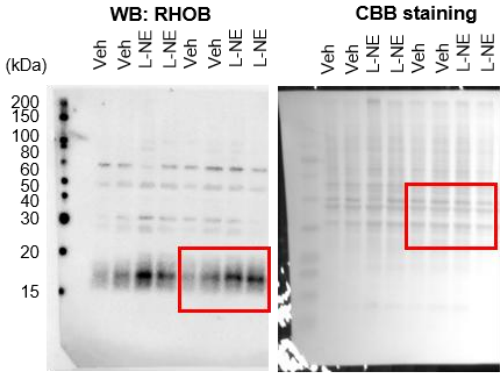

Supplementary Figure 7

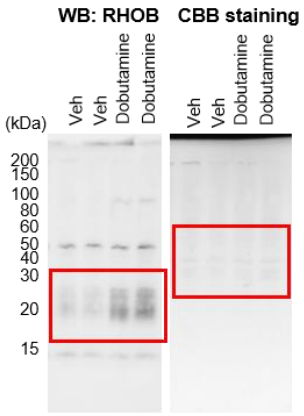

Fig. 2F Western blots full membranes

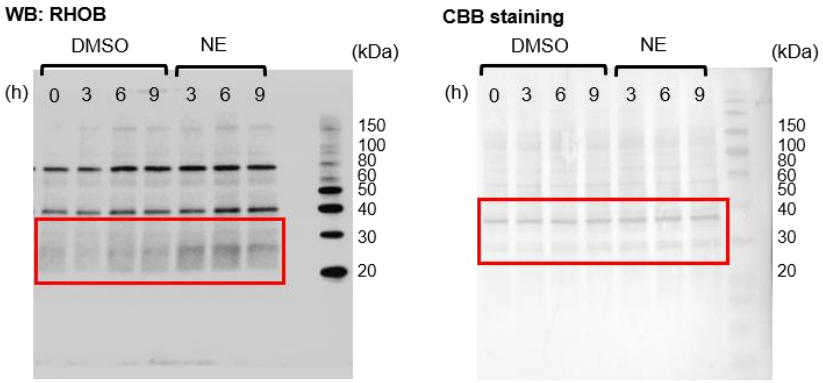

Fig. 5B Western blots full membranes
Supplementary Figure 11 Western blots full membranes

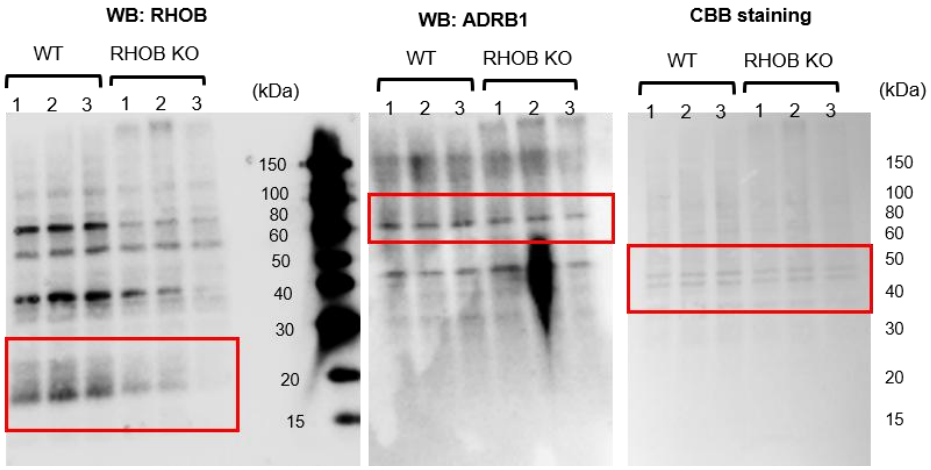

Supplementary Figure 5: Uncropped Western blot membranes corresponding to the main figures.

Full, uncropped images of the Western blot membranes and corresponding total protein staining used for the analyses presented in Fig. 2, Fig. 5, and Supplementary Figure 9. Red boxes indicate the regions displayed in the corresponding cropped panels of the main figures. Molecular weight markers are shown where applicable.

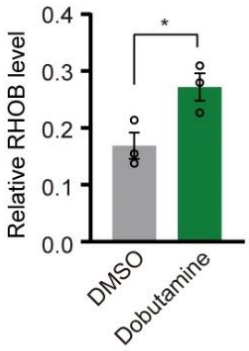

Supplementary Figure 6: β1-AR activation induced RHOB protein expression in the iHTMC.

WB revealed that RHOB levels were significantly elevated by 6 hours of β1-AR agonist dobutamine (unpaired Welch's *t*-test, $*p < 0.05$). Data are presented as bar graphs (mean ± SEM) with scatter plot of independent experiments (n = 3).

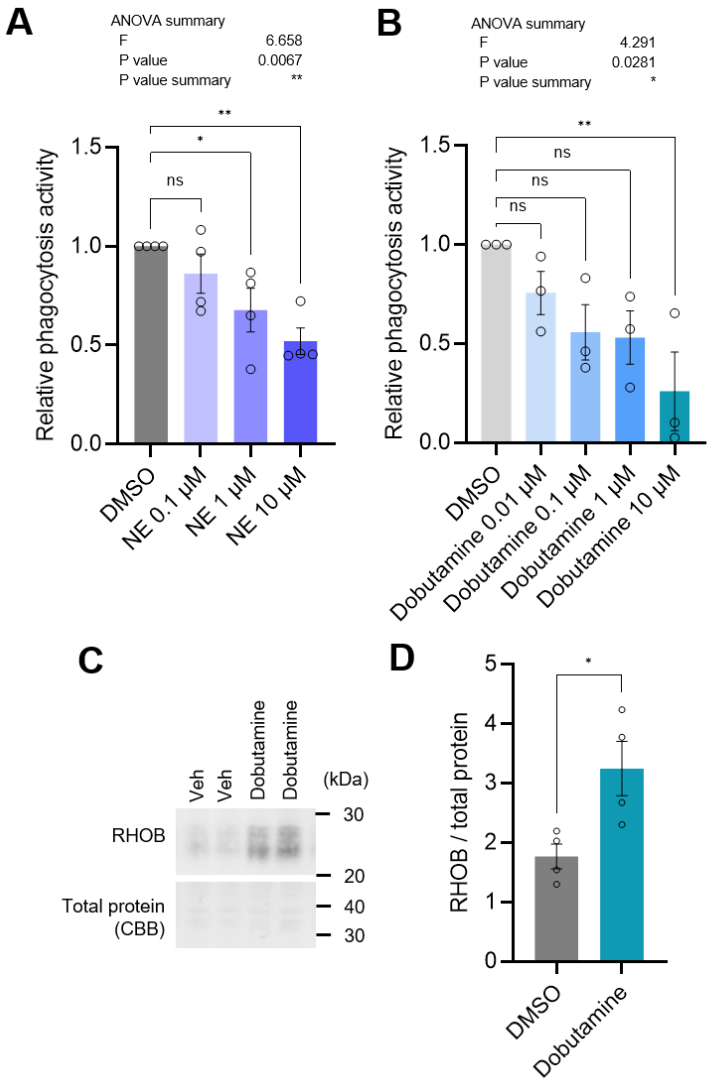

Supplementary Figure 7: Validation of norepinephrine and dobutamine responses in primary human trabecular meshwork cells.

(**A, B**) Phagocytic activity of primary HTMC cells following exposure to NE (**A**) or dobutamine (**B**). Both NE and dobutamine reduced phagocytic activity in a dose-dependent manner (*p < 0.05, **p < 0.01, one-way ANOVA followed by Dunnett's multiple-comparison test [p < 0.05]). Data are presented as mean ± SEM with individual biological replicates (n = 4 [**A**], n = 3 [**B**]) (**C**) Representative Western blot showing RHOB protein expression in primary HTMCs following treatment with 6h dobutamine (1 µM). (**D**) Quantification of RHOB protein expression shown normalized with total protein (CBB) in (**C**). Dobutamine increased RHOB levels in primary HTMCs (*p < 0.05, Welch's t-test). Data are presented as mean ± SEM with individual biological replicates (n = 4).

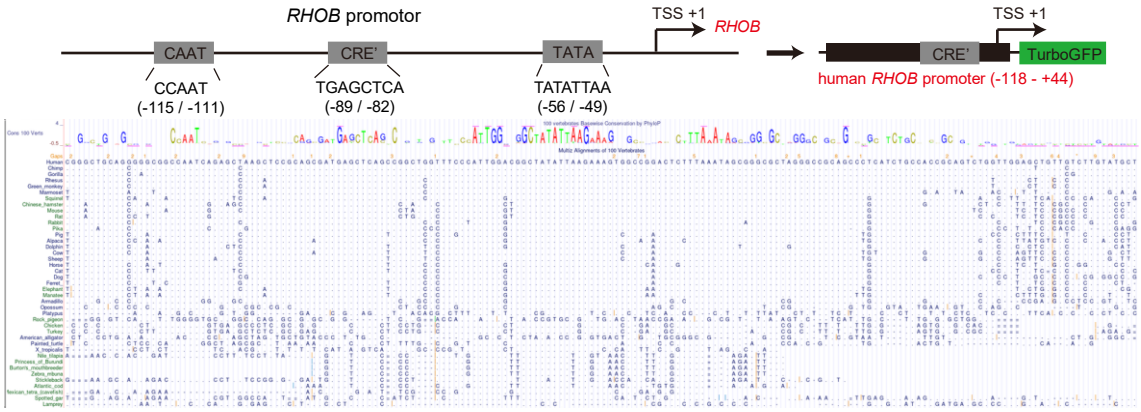

Supplementary Figure 8: Identification of a putative cAMP-responsive element (CRE) in the human RHOB promoter.

Annotation analysis of the human *RHOB* promoter region (−1,500 to +1 bp relative to the transcription start site [TSS]) using the UCSC Genome Browser. Predicted regulatory elements, including a TATA box, CAAT box, and a previously unrecognized CRE-like motif (CRE′; TGAGCTCA), are indicated. The CRE′ site is located proximal to the TSS and was subsequently investigated as a candidate mediator of β1AR–cAMP–CREB-dependent transcriptional regulation of *RHOB*.

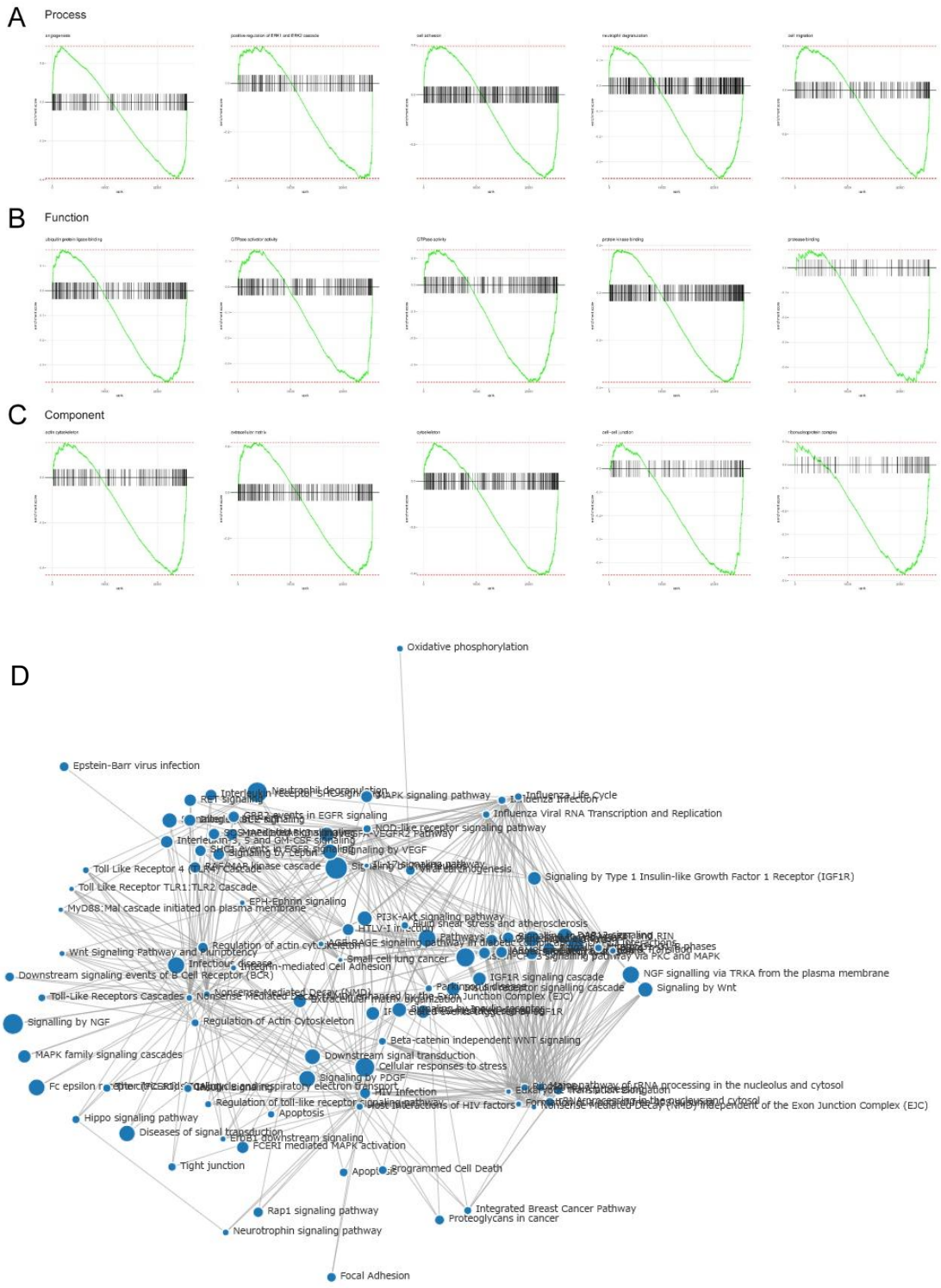

Supplementary Figure 9: RUG plots of Gene set enrichment analysis (GSEA) and Network diagram of the gene ontology terms of NE-treated iHTMC.

(**A-C**) The running score plot of the first top five terms identified on differentially expressed genes upon 6 h - NE treatment. The x-axis is the ranked genes based on their score and the y-

axis is their enrichment score; biological process (**A**), molecular function (**B**), and cellular component (**C**). The rug in the x-axis indicates the genes with the corresponding NE-induced TM phenotype changes. The positions of maximum and minimum running enrichment score were denoted by a red dashed line. (**D**) Network diagram of the gene ontology terms. Circle size indicates the number of genes.

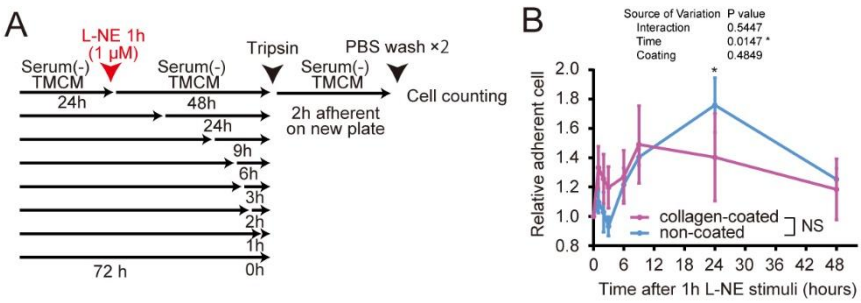

Supplementary Figure 10: Transient NE stimulation to iHTMC enhances cell adhesion time-dependently

(**A**) iHTMCs were exposed to NE for 1 hour before detachment of cells by trypsin (0, 1, 3, 6, 9, 12, or 24 hours before), and cultured to adhere to new dishes (collagen-coated or uncoated) for 2 hours after suspension, and then measured adherent cells using a cell counting kit. (**B**) Cell adhesion assay revealed that transient L-NE stimulation (1 h) induced cell adhesion time-dependently (* $p < 0.05$ vs. 0h, Dunnett's multiple comparison test, two-way ANOVA [Time; * $p = 0.0147$]). Coating showed no effect (two-way ANOVA [coating; $p = 0.4849$]). Data are normalized by 0-hour cell numbers and presented as line graphs (mean ± SEM) of independent experiments (n = 3).

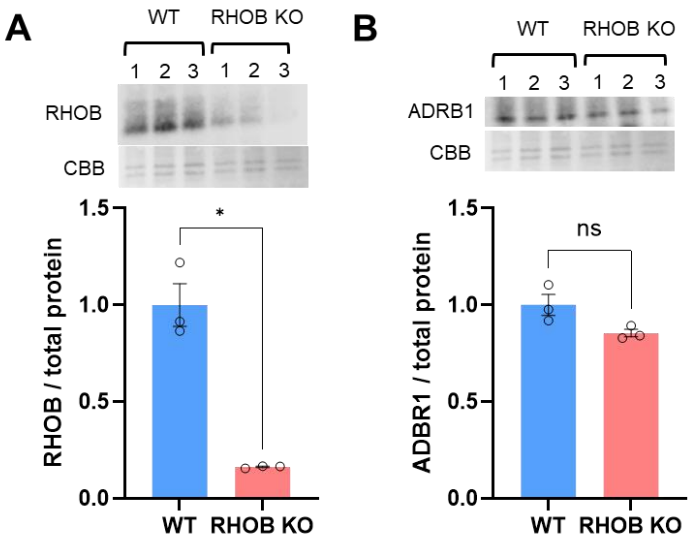

Supplementary Figure 11: Validation of RHOB-deficient iHTMCs and assessment of ADRB1 expression.

Quantitative RT-PCR analysis of RHOB (**A**) and ADRB1 (**B**) expression in WT and CRISPR/Cas9-generated polyclonal RHOB-deficient iHTMCs (RHOB KO). (**A**) RHOB expression was significantly reduced in KO cells, confirming successful gene disruption. RHOB-deficient cells were generated as a CRISPR/Cas9-edited polyclonal population; therefore, residual RHOB expression is attributable to incomplete editing across individual cells. (**B**) ADRB1 protein expression was not significantly altered, indicating that the reduced responsiveness observed in KO cells is unlikely to be explained by changes in β1AR expression. Protein levels were normalized to total protein (CBB stained). Data are presented as mean ± SEM with individual biological replicates (n = 3). Statistical significance was determined using an unpaired Welch's *t*-test. **p* < 0.05; ns, not significant.

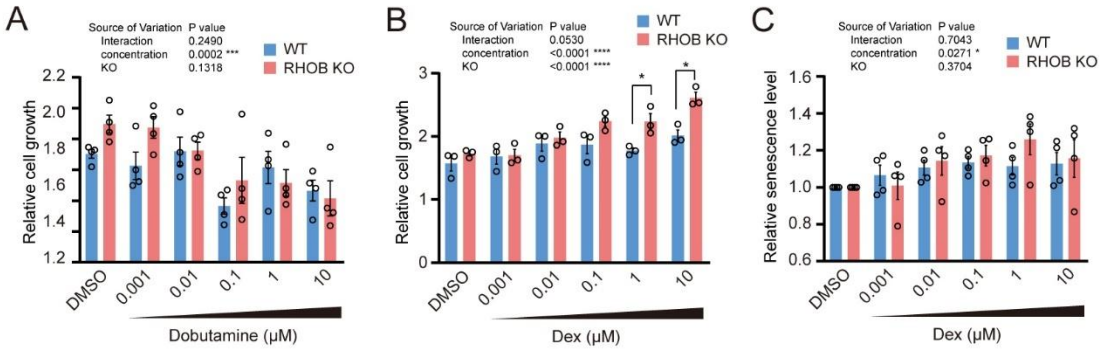

Supplementary Figure 12: Effects of RHOB KO and Dex on cell growth and senescence.

(**A**) Effect of dobutamine on cell growth. Incubation for 48 hours with serum (+) medium induced iHTMC growth, but β1-AR agonist dobutamine dose-dependently inhibited the cell growth (Two-way ANOVA [concentration; *** $p = 0.0002$]), while RHOB KO showed no effect (Two-way ANOVA [KO; $p = 0.1318$]). (**B**) Two-day incubation with serum (+) medium induced iHTMC growth, but dexamethasone (Dex) dose-dependently enhanced the cell growth (Two-way ANOVA [concentration; **** $p < 0.0001$]), while RHOB KO slightly increased Dex-induced cell growth under high concentration of Dex (* $p < 0.05$ vs. WT, Šidák multiple comparison test, two-way ANOVA [KO; **** $p < 0.0001$]). Data are normalized by 0-day cell numbers and presented as bar graphs (mean ± SEM) with scatter plots of independent experiments (n = 3 [**B**], n = 4 [**A**]). (**C**) Incubation for 96 hours with serum free medium with Dex slightly induced iHTMC senescence dose-dependently (Two-way ANOVA [concentration; * $p = 0.0271$]), while RHOB KO showed no effect (Two-way ANOVA [KO; $p = 0.3704$]). Data are normalized by signals of DMSO-treated cells and presented as bar graphs (mean ± SEM) with scatter plot of independent experiments (n = 4).

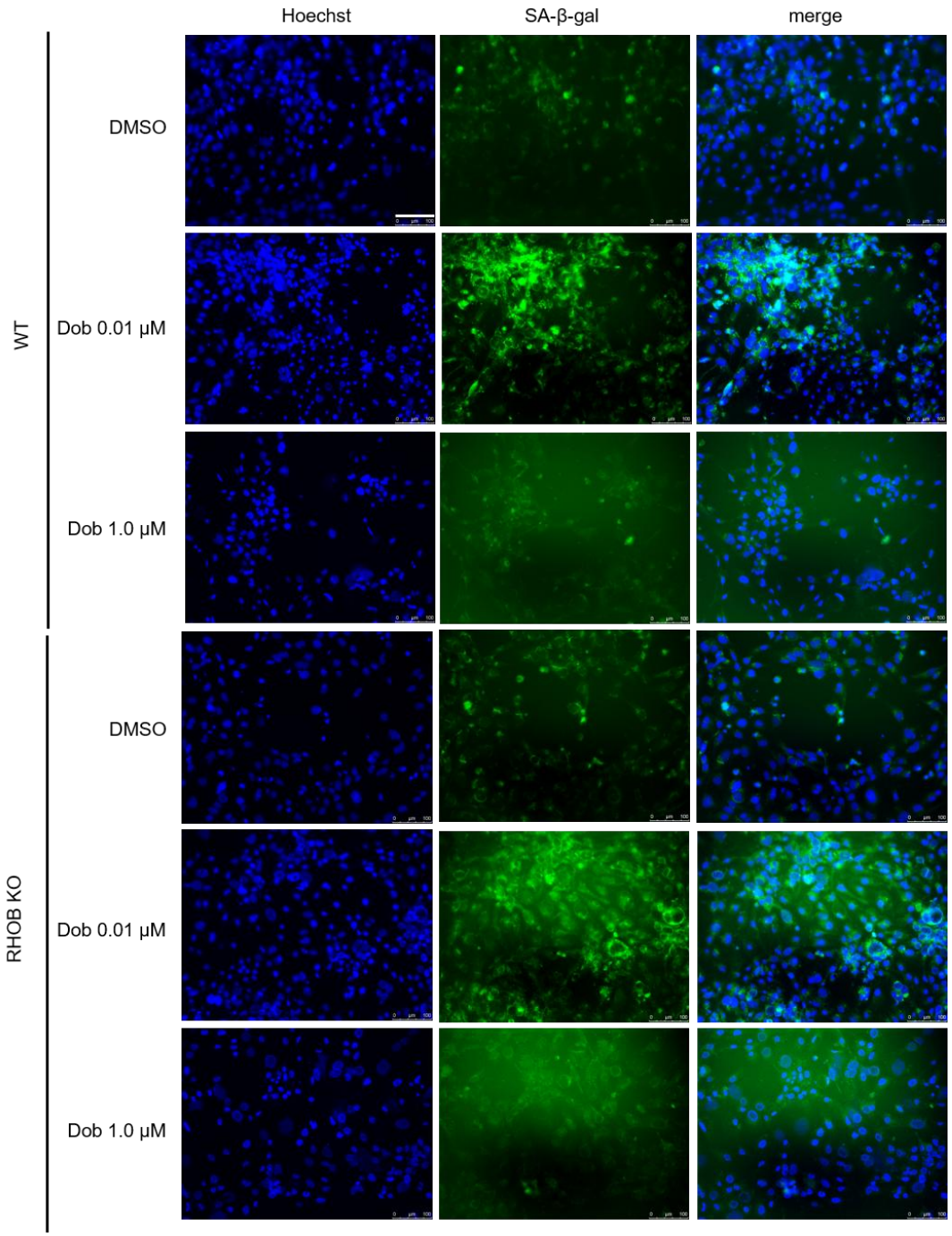

Supplementary Figure 13: Representative senescence-associated β-galactosidase staining in WT and RHOB-deficient TM cells.

Representative images of senescence-associated β-galactosidase (SA-β-gal) staining in WT and CRISPR/Cas9-generated polyclonal RHOB-deficient iHTMCs treated with vehicle (DMSO), low-dose dobutamine (0.01 µM), or high-dose dobutamine (1 µM) for 6 h. SA-β-gal-positive cells are shown in green, and nuclei were counterstained with Hoechst (blue). Merged images are shown in the right panels. Images correspond to the quantitative senescence analyses presented in Fig. 5E and are representative of three independent experiments. Scale bar, 100 µm.

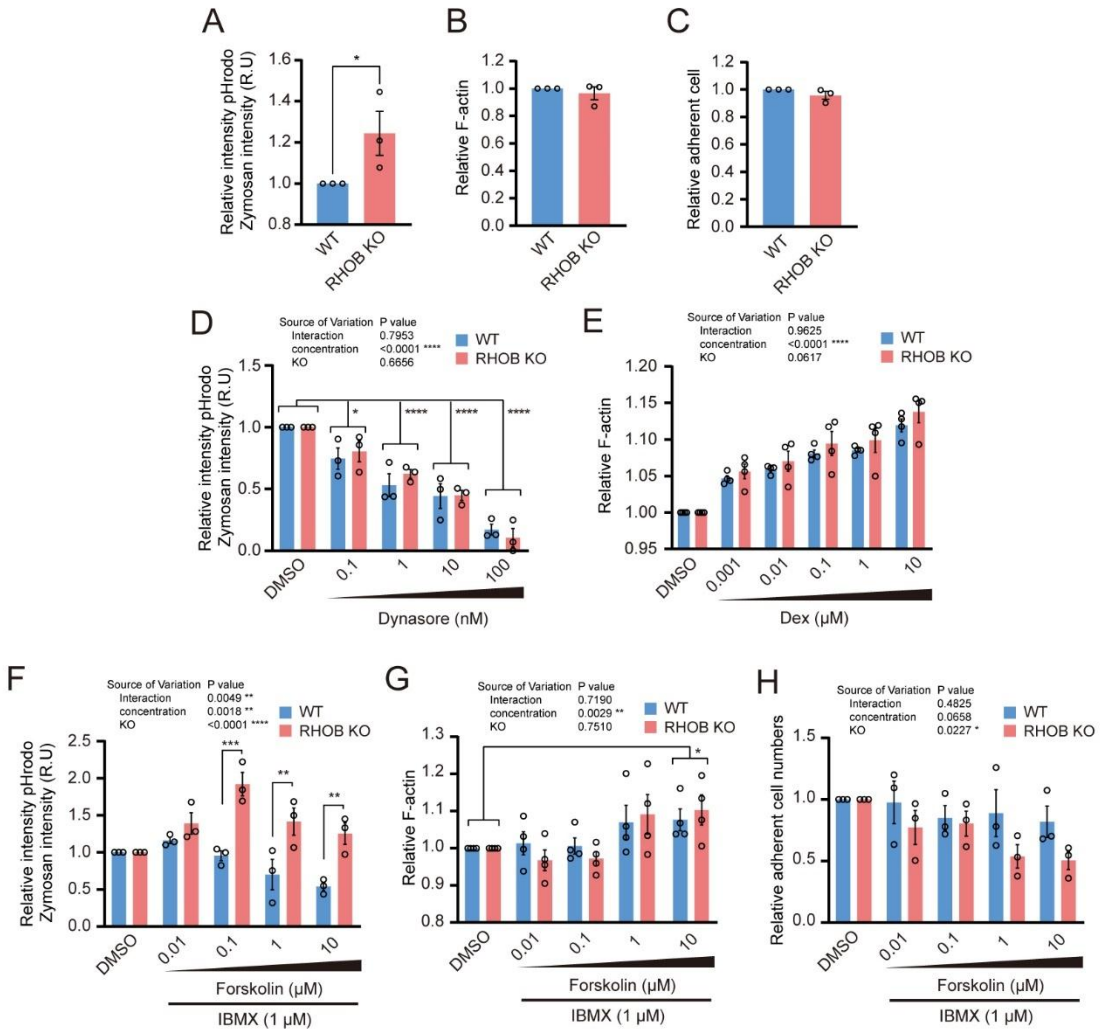

Supplementary Figure 14: The role of RHOB in iHTMC physiological functions

(**A-C**) Effects of RHOB KO on iHTMC phagocytosis (**A**), actin polymerization (**B**), and cell adhesion (**C**). **A** RHOB KO significantly enhanced TM phagocytotic activity (unpaired *t*-test, * $p < 0.05$), while RHOB KO showed no effect on (**B**) actin polymerization and (**C**) cell adhesion (unpaired Welch's *t*-test; $p > 0.05$]). (**D**) Incubation for 6 hours with dynamin inhibitor dynasore suppressed TM phagocytosis dose-dependently (* $p < 0.05$, **** $p < 0.0001$ vs. DMSO, Dunnett's multiple comparison test, Two-way ANOVA [concentration; **** $p < 0.0001$]), while RHOB KO showed no effect (two-way ANOVA [KO; $p = 0.6656$]). (**E**) Incubation for 96 hours with serum free medium with Dex slightly induced iHTMC actin-polymerization dose-dependently (**** $p < 0.0001$ vs. DMSO, Dunnett's multiple comparison test, Two-way

ANOVA [concentration; **** $p < 0.0001$]), while RHOB KO showed no effect (Two-way ANOVA [KO; $p = 0.0617$]). (**F-H**) Effects of RHOB KO and cAMP inducers on iHTMC physiological functions. (**F**) cAMP inducers (IBMX and forskolin) suppressed TM phagocytosis, but in RHOB KO cells, high cAMP inducers clearly rescued phagocytosis as we expected and low cAMP inducers dramatically increased TM phagocytotic activity (** $p < 0.01$, *** $p < 0.001$ vs. WT, Šidák multiple comparison test, two-way ANOVA [concentration; *** p = 0.0018, KO; **** $p < 0.0001$]). (**G**) cAMP inducers gradually raised TM F-actin level, but RHOB KO showed no effect (* $p < 0.05$ vs. DMSO, Dunnett's multiple comparison test, Two-way ANOVA [concentration; ** $p = 0.0029$]). (**H**) RHOB KO slightly decreased TM senescence at high cAMP inducers (Two-way ANOVA [KO; * $p = 0.0227$]). Data are normalized by signals of DMSO-treated cells and presented as bar graphs (mean ± SEM) with scatter plot of independent experiments (n = 3 [**A**, **B**, **C**, **D**, **F**, **H**], n= 4 [**E**, **G**]).

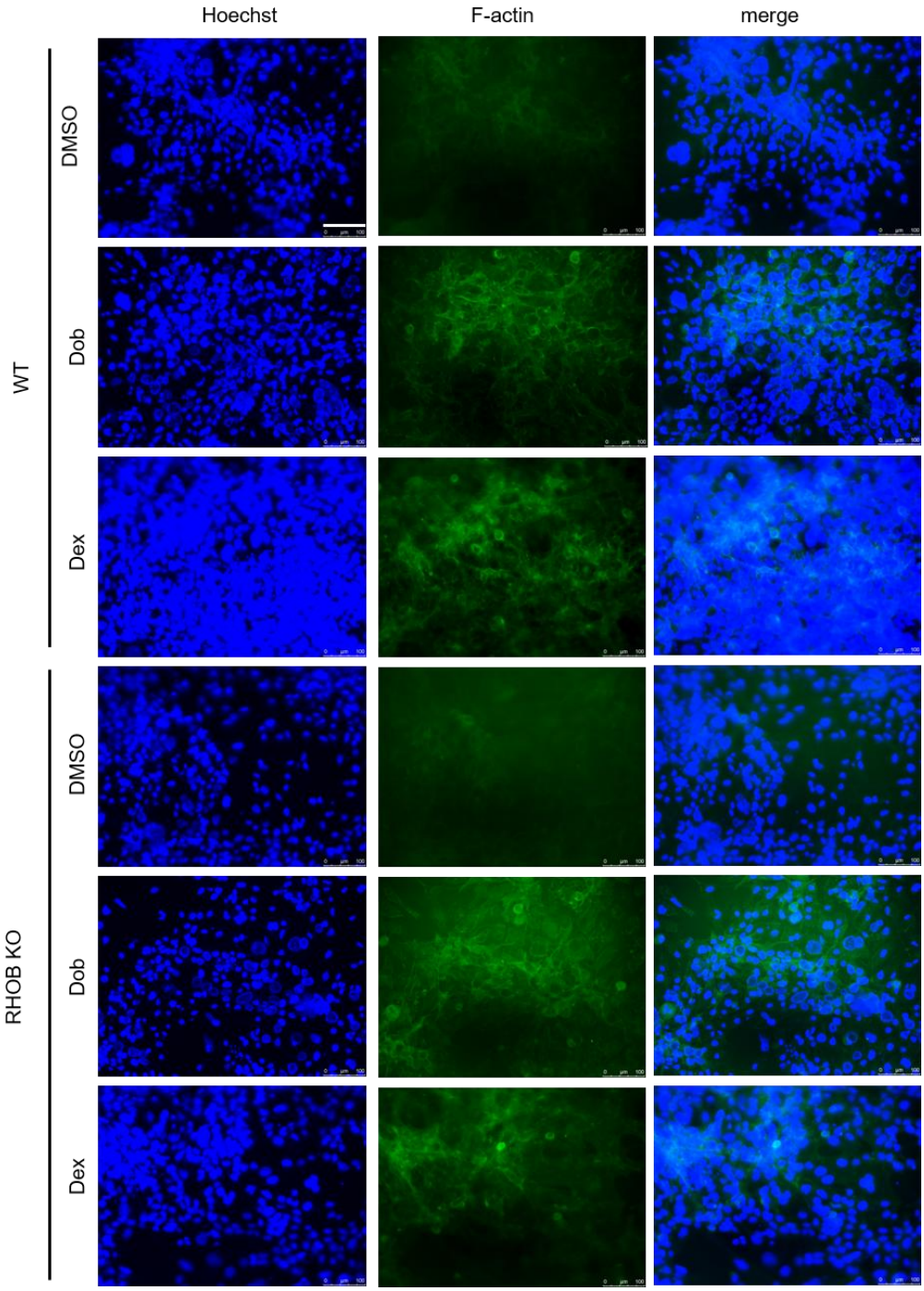

Supplementary Figure 15: Representative F-actin staining in WT and RHOB-deficient TM cells following β-adrenergic or glucocorticoid stimulation.

Representative phalloidin staining images showing F-actin organization in wild-type (WT) and CRISPR/Cas9-generated polyclonal RHOB-deficient iHTMCs treated with vehicle (DMSO), dobutamine (Dob), or dexamethasone (Dex) for 6 h. F-actin is shown in green and nuclei are counterstained with Hoechst (blue). Merged images are shown in the right panels. Images correspond to the quantitative analyses presented in Fig. 5G and are representative of three independent experiments. Scale bar, 100 µm.

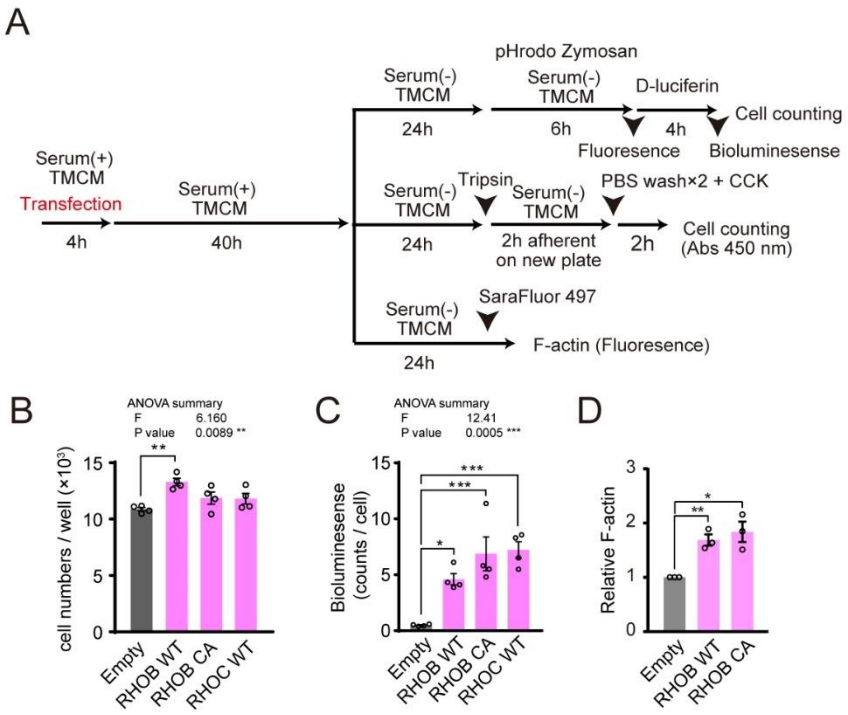

Supplementary Figure 16: Effects of RHOB overexpression on TM cellular physiology

(**A**) Transfection to RHOB overexpression in the iHTMC were performed to monitor TM phagocytotic activity using pH senser (pHrodo)-zymosan, cell adhesion assay, and actin polymerization (fibrillation) using SaraFluor 497 F-actin probe. (**B**) RHOB WT overexpression slightly increased cell numbers (one-way ANOVA [** $p = 0.0089$]). Data are presented as bar graphs (mean ± SEM) with scatter plot of independent experiments (n = 4). (**C**) Transfected cells showed bioluminescence because of plasmid Nluc constructs (* $p < 0.05$, *** $p < 0.001$, one-way ANOVA [*** $p = 0.0005$]). Data are presented as bar graphs (mean ± SEM) with scatter plots of independent experiments (n = 3-4). (**D**) RHOB WT and CA transfected cells showed an increase in actin polymerization (* $p < 0.05$, ** $p < 0.01$, one-way ANOVA [*** $p < 0.001$]). Data are presented as bar graphs (mean ± SEM) with scatter plots of independent experiments (n = 3).

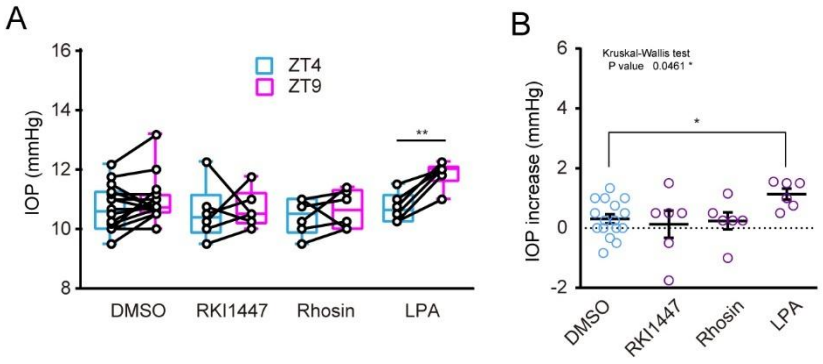

Supplementary Figure 17: RHO activator LPA induced day-time IOP increase in mice

(**A**) Instillation of RHO activator lysophosphatidic acid (LPA) to mice eye during day slightly but significantly induced IOP increase (more than 1 mmHg) 5 hours after (paired *t*-test, ** $p < 0.01$ ZT4 vs. ZT9), but ROCK inhibitor (RKI1447) and RHO inhibitor Rhosin did not. Data are presented as box-and-whisker plots with individual data (n = 6 [RKI1447, Rhosin, LPA], 16 [DMSO]). (**B**) Individual analysis indicated LPA-induced IOP (* $p < 0.05$ vs. DMSO, Dunnett's multiple comparison test, one-way ANOVA [* $p = 0.0461$]). Data are presented as scatter plots with mean ± SEM (n = 6 [RKI1447, Rhosin, LPA], 16 [DMSO]).

Gene	Forward primer (5′–3′)	Reverse primer (5′–3′)	Product size (bp)	Primer bank ID
Rhob	GTGCCTGCTGATCGTGTTCA	CCGAGAAGCACATAAGGATGAC	200	6680726a1
Per1	TGAAGCAAGACCGGGAGAG	CACACACGCCGTCACATCA	143	24980945a1
Gprc5a	TTGCATGTTTGCACTCGTTTTC	GCCAAAGACCCCTAGCACT	109	225543464c2
Rgs2	GAGAAAATGAAGCGGACACTCT	GCAGCCAGCCCATATTTACTG	197	31543586a1
Atf3	GAGGATTTTGCTAACCTGACACC	TTGACGGTAACTGACTCCAGC	110	31542154a1
Nr4a3	AGGATTCACTGATCTCCCCAA	GATGCAGGACAAGTCCATTGC	140	7657397a1
Nr4a2	GTGTTCAGGCGCAGTATGG	TGGCAGTAATTTCAGTGTTGGT	153	7305325a1
Ifrd1	CGAAGAACAAGAAGCGGAACG	AAGGTTGAACAGTCCGATGCG	111	226062272c1
Cebpd	CGACTTCAGCGCCTACATTGA	GAAGAGGTCGGCGAAGAGTT	82	110665734c1
Avpi1	CCCTGTGGCAGGTTTCAACA	CCTCAGCTACACGGTGATCC	177	19526465a1
Gadd45b	CAACGCGGTTCAGAAGATGC	GGTCCACATTCATCAGTTTGGC	122	6678980a1
Dusp1	GTTGTTGGATTGTCGCTCCTT	TTGGGCACGATATGCTCCAG	129	7305423a1
Rasd1	GATGTGCCCAAGCGACTCT	TGAGGAAGCGCGACACAAT	110	6677673a1
Rgs16	GGTACTTGCTACTCGCTTTTCC	CAGCCGCGTCTTGAACTCT	151	29437173a1
Fosb	CGAGAAGAGACACTTACCCCA	GTTTCCGCCTGAAGTCGATCT	125	110350004c2
Cyp1b1	CACCAGCCTTAGTGCAGACAG	GAGGACCACGGTTTCCGTTG	144	6753568a1
Btg2	ATGAGCCACGGGAAGAGAAC	GCCCTACTGAAAACCTTGAGTC	122	6680814a1
Arc	AAGTGCCGAGCTGAGATGC	CGACCTGTGCAACCCTTTC	105	9055166a1
Hprt	CATTATGCTGAGGATTTGGAAAGG	CTTGAGCACACAGAGGGCTACA	129	
RHOB	ATCCCCGAGAAGTGGGTCC	CGAGGTAGTCGTAGGCTTGGA	190	42716309c2
HPRT1	CCTGGCGTCGTGATTAGTGAT	AGACGTTCAGTCCTGTCCATAA	131	164518913c1

Supplementary Table 1: qPCR primers list

Supplementary Methods

Primary human trabecular meshwork cell culture

Primary human trabecular meshwork cells (HTMCs; #6590, ScienCell Research Laboratories, Carlsbad, CA, USA) were cultured in trabecular meshwork cell medium (TMCM; #6591, ScienCell) supplemented with 1% fetal bovine serum (#0010, ScienCell), 1% trabecular meshwork cell growth supplement (TMCGS; #6592, ScienCell), and 1% penicillin/streptomycin (#0503, ScienCell). Cells were maintained on type I collagen-coated culture dishes or plates at 37 °C in a humidified atmosphere containing 5% CO_2.

For experiments, HTMCs were seeded onto type I collagen-coated plates and cultured to confluence. The medium was then replaced with serum-free TMCM for 24 h before treatment. Cells were exposed to norepinephrine (NE; 0.1, 1, and 10 μM) or dobutamine (0.01, 0.1, 1, and 10 μM) at the indicated concentrations and durations. Phagocytosis assays and RHOB expression analyses were subsequently performed as described above. Primary HTMCs were used at early passages according to the manufacturer's recommendations.

Inhibition of transcription

To address the importance of genomic regulation in NE-suppressed TM phagocytosis, we added transcription inhibitor cordycepin (1, 0.1, 0.001, 0.0001 μM; FIJIFILM WAKO, #WK03122731) with dobutamine (1 μM) to measured phagocytosis activity using pHrodo zymosan green pHrodo Green Zymosan Bioparticles (P35365; ThermoFisher) as previous report [1]. Cordycepin administration partially rescued dobutamine-induced TM phagocytosis suppression.

qRT-PCR

Total RNA was isolated from iHTMC utilizing the NucleoSpin RNA/Protein kit (U0933A, Takara Bio Inc., Japan), following the manufacturer's protocol. Genomic DNA was subsequently removed through DNase I treatment (Toyobo, Osaka, Japan). A 0.5 μg aliquot of each total RNA sample was employed for direct qRT-PCR. The qRT-PCR was conducted using an ABI QuantStudio1 in a total reaction volume of 10 μL, with the RNA-direct™ SYBR ® Green Realtime PCR Master Mix (QRT-201, Toyobo), in accordance with the supplier's guidelines. mRNA quantification was achieved using two primers (Integrated DNA Technologies), as detailed in Supplementary Table 1. The threshold cycle (Ct) values obtained from the cDNA amplifications were normalized against the Ct values for *Hprt* or *HPRT1* using standard procedures.

Enrichment analysis

To find the important terms related to 18 upregulated genes by NE stimuli, we performed KEGG pathway analysis, Tabula Sapiens analysis, and Jensen TISSUES analysis using web tool Enrichr (https://maayanlab.cloud/Enrichr/) and made graphs using web tool Srplots (https://www.bioinformatics.com.cn/en). GSEA (gene set enrichment analysis) and its RUG plots of NE-treated iHTMC (GSE336386) were conducted by RaNAseq (https://ranaseq.eu/index.php).

Cell growth

iHTMCs (#T0371, abm) were plated in collagen I-coated 96-well microplates (#4860-010; IWAKI) at a density of 2.5×10^3 cells/well in trabecular meshwork cell medium (TMCM) supplemented with 1% penicillin/streptomycin and growth factors (#6591; Sciencell). After 48 h, 10 μL of cell counting kit-8 (CCK-8, Dojindo Laboratories, CK04) was added to cells seeded in

96 wells, and incubated for 1 h in a 37 °C CO_2 incubator. To calculate cell numbers, iHTMC were preincubated in collagen I coated 96-well microplates (4860-010; IWAKI) at densities of 16×10^3, 8.0×10^3, 4.0×10^3, 2.0×10^3, 1.0×10^3, and 0.5×10^3 cells/well with serum free TMCM (1% penicillin/streptomycin; #6591; Sciencell), and were counted as standard. Subsequently, the absorbance (450 nm) was measured using a Nivo microplate reader (PerkinElmer, #HH3500).

Subsequently, at the time of medium replacement, Dobutamine (Sigma-Aldrich, #D0676) and Dex (Dexamethasone, Sigma-Aldrich, #D4902) were added to the serum-(+) TMCM at final concentrations of 0, 0.001, 0.01, 0.1, 1, and 10 μM. The medium was then replaced. The effect of these compounds on the cell proliferation rate was assessed using Cell Counting Kit-8.

Cell adhesion assays

iHTMCs were plated in collagen I-coated 96-well microplates (#4860-010; IWAKI) at a density of 5×10^3 cells/well in serum (+) TMCM (#6591; Sciencell). After 100 % confluency, medium was changed to serum free TMCM for 24 h. Then, dobutamine and Dex were added to the serum (+) TMCM at final concentrations of 0, 0.001, 0.01, 0.1, 1, and 10 μM. After 8 h, iHTMCs were washed once with PBS, detached with 30uL of 0.25 % trypsin treatment for 5 mins and diluted with 170μL of serum (+) TMCM. The entire volume was seeded onto new collagen-coated 96-well plate (#4860-010; IWAKI), placed in a CO_2 incubator for 2 hours, washed twice with PBS, and quantified for adherent cells as described above. The adhesion rate was calculated as the ratio of the absorbance of treated samples to the control wells.

After 72 h of fluorescent measurement, 10 μL of cell counting kit-8 (CK04, Dojindo) was added to cells seeded in quadruplicate in 96 wells, and incubated for 4 h in a 37 °C CO_2

incubator. To calculate cell numbers, iHTMC were preincubated in collagen I coated 96-well microplates (4860-010; IWAKI) at densities of 16×10^3, 8.0×10^3 , 4.0×10^3, 2.0×10^3, 1.0×10^3, and 0.5×10^3 cells/well with serum free TMCM (1% penicillin/streptomycin; #6591; Sciencell), and were counted as standard. Subsequently, the absorbance (450 nm) was measured using a Nivo (PerkinElmer).

β-galactosidase assays

To measure SA-β-galactosidase (senescent cell marker), we used the Cellular Senescence Detection Kit -SPiDER-βGal protocol (#SG02, DOJINDO), following the manufacturer's instructions. Briefly, dobutamine and Dex at final concentrations of 0, 0.001, 0.01, 0.1, 1, and 10 μM were added 1 day after the medium was changed to serum-free TMCM. After 6 h, dobutamine-treated iHTMC were incubated with SPiDER-βGal working solution (1 : 1,000) at 37 °C for 30 min after washing twice with Hanks‘Balanced Salt Solution (HBSS; 082-08961 WAKO). For Dex, iHTMC were exposed with Dex after 96 h. After washing once with HBSS, fluorescence (Ex = 500 nm; Em = 540 nm) was measured using a Nivo (PerkinElmer).

For imaging, iHTMCs were seeded into 8-well chambered glass slides (#192-008, WATSON) and cultured to confluence with serum (+) TMCM. Cells were serum-starved overnight and subsequently treated with dobutamine (0, 0.01, or 1 μM) together with SPiDER-βGal working solution (1:1,000; Cellular Senescence Detection Kit - SPiDER-βGal, #SG02, DOJINDO) in serum-free TMCM. After 6 h of incubation at 37 °C, cells were washed twice with HBSS and counterstained with DAPI. Fluorescence images were acquired using a Leica fluorescence microscope. SA-β-gal activity was visualized in the FITC channel (Ex/Em ≈ 500/540 nm), and representative images are shown in Supplementary Figure 13.

Actin polymerization assay

For imaging, WT and RHOB KO iHTMCs were seeded into an 8-well chamber slide (#192-008, WATSON) and cultured to confluence with serum (+) TMCM. After overnight serum starvation, cells were treated with vehicle (DMSO), 1 μM dobutamine, or 100 nM dexamethasone (Dex) in serum-free TMCM. Six hours after dobutamine or Dex treatment, cells were washed with HBSS and stained with 100 nM SaraFluor 497 actin probe (AR5601-N5, Goryo Chemical, Inc., Japan). Nuclei were counterstained with Hoechst. Fluorescence images were acquired using a Leica fluorescence microscope. Representative images illustrating actin filament organization following β-adrenergic or glucocorticoid stimulation are shown in Supplementary Figure 15.

Analysis of gene expression using Public Data

We performed data analysis of gene expression in human AH outflow-related cells from the Gene Expression Omnibus accession number GSE146188 [2]. Data can be visualized in the Broad Institute's Single Cell Portal at https://singlecell.broadinstitute.org/single_cell/study/SCP780.

RHOB overexpression

We seeded iHTMCs in 2 mL of serum (+) TMCM in a collagen-coated 6 well one day before transfection to achieve 50–70% confluency at the time of transfection. To express RHO protein in iHTMC, we designed pcDNA3.1+ plasmids inserted Nano luciferase-combined to N-terminal of wild-type (WT) RHOB and RHOC as control, and constitutive acrtive (CA) RHOB. We dilute 1 μg of these plasmid DNAs in 50 μL of Xfect Reaction Buffer (Takara Bio, # 631318), and then add 0.3 μL of Xfect Polymer to the diluted DNA. After 10 min incubation at

room temperature to form the transfection complex, the prepared transfection complex dropwise was gently added to each well. After 4 hours incubation at at 37°C in a humidified incubator with 5% CO_2, we replaced the transfection medium with fresh growth medium and incubated to recover and express RHOB for 48 hours.

For validation of RHOB expression, we added the substrate for Nluc (99-325-50, NanoLight technology) to the culture medium as per the reagent's instructions, and measured the luminescence using a microplate reader Nivo (Perkin Elmer) to compare luminescence intensity between the experimental group (RHOB WT, RHOB CA, or RHOC WT plasmid) and controls (empty vector). After validation, we confirmed cell growth, phagocytotic activity, actin polymerization, cell adhesion, liquid permeability, and then investigated the effect of RHO inhibitor Rhosin on RHOB overexpression-suppressed TM phagocytosis level.

LPA instillation and IOP measurement

After IOP measurement, instillation of ROCK inhibitor (RKI1447; 1 mM), RHO inhibitor Rhosin (1 mM), RHO activator lysophosphatidic acid (LPA; 1 mM; FIJIFILM) to mice eye (n = 6-16) was performed at ZT4. Five hours after, we measured IOP again at ZT9 to detect the increasing effects.

Supplementary References

1. Ikegami, K. & Masubuchi, S. Suppression of trabecular meshwork phagocytosis by norepinephrine is associated with nocturnal increase in intraocular pressure in mice. *Communications Biology* **5**, 339 (2022).
2. van Zyl, T. *et al.* Cell atlas of aqueous humor outflow pathways in eyes of humans and four model species provides insight into glaucoma pathogenesis. *Proceedings of the National*

Academy of Sciences of the United States of America **117**, 10339–10349 (2020).